REPORT DOCUMENTATION PAGE

Form Approved

OMB No. 0704-0188

1. REPORT DATE *(DD-MM-YYYY)*	2. REPORT TYPE	3. DATES COVERED *(From - To)*
20-03-2015	Final	20140115- 20150114

4. TITLE AND SUBTITLE

First Principles Study of Band Structure and Band Gap Engineering in Graphene for Device Applications

5a. CONTRACT NUMBER
FA2386-14-1-4007

5b. GRANT NUMBER
Grant AOARD-144007

5c. PROGRAM ELEMENT NUMBER
61102F

6. AUTHOR(S)

Dr Kombiah Thevar Iyakutti

5d. PROJECT NUMBER

5e. TASK NUMBER

5f. WORK UNIT NUMBER

7. PERFORMING ORGANIZATION NAME(S) AND ADDRESS(ES)
SRM UNIVERSITY
KANCHIPURAM,
TAMILNADU 603203 INDIA

8. PERFORMING ORGANIZATION REPORT NUMBER
N/A

9. SPONSORING/MONITORING AGENCY NAME(S) AND ADDRESS(ES)

AOARD
UNIT 45002
APO AP 96338-5002

10. SPONSOR/MONITOR'S ACRONYM(S)
AFRL/AFOSR/IOA(AOARD)

11. SPONSOR/MONITOR'S REPORT NUMBER(S)
AOARD-144007

12. DISTRIBUTION/AVAILABILITY STATEMENT

Distribution Code A: Approved for public release, distribution is unlimited.

13. SUPPLEMENTARY NOTES

14. ABSTRACT In the last decade, graphene research has emerged as a promising candidate for numerous semiconductor and other device applications. The main challenge in graphene is the opening of the band gap in the semimetallic electronic structure. In the bandstructure of graphene which is dominated by Dirac description, valence and conduction bands cross the Fermi level at a single point (K points) in the Brillouin zone and hence it is a is a zero gap semiconductor or a semimetal with zero density of states . Due to the linear dispersion of energy bands and appearance of Dirac cones near the 'K' point and Fermi level the electrons behave like massless Dirac fermions. For applications in nanoelectronic devices a suitable band gap is essential. This report examines by firstr principles calculation the behavior of graphene with vacancies and with various dopants introduced to occupy vacancies. The result is improved semiconductor behavior and more sustainable, cost effective functionalized graphene.

15. SUBJECT TERMS

NDE, Finite Difference Methods, Carbon Fiber composites

16. SECURITY CLASSIFICATION OF:			17. LIMITATION OF ABSTRACT	18. NUMBER OF PAGES	19a. NAME OF RESPONSIBLE PERSON
a. REPORT	b. ABSTRACT	c. THIS PAGE			David Hopper, Lt Col, USAF, Ph.D.
U	U	U	SAR	31	**19b. TELEPHONE NUMBER** *(Include area code)* +81-42-511-2000

ASIAN OFFICE OF AEROSPACE RESEARCH AND DEVELOPMENT(AOARD)

Final Performance Report

(Grant FA2386-14-1-4007)

First Principles Study of Band Structure and Band Gap Engineering in Graphene for Device Applications

Dr. K. Iyakutti
Professor-Emeritus &
Principal Investigator AOARD Project
Department of Physics and Nanotechnology
SRM University, SRM Nagar, Kattankulathur
Chennai,Tamilnadu - 603203, INDIA
(iyakutti.k@ktr.srmuniv.ac.in ; iyakutti@gmail.com)

Objectives

To investigate: 1) Substitutional doping in graphene;
2) Functionalization with oxygen like atoms;
3) Strain-induced band gap opening in graphene;
4) Band gap opening and modulation in graphene with mono and di-vacancies;
5) Consolidation of results.

Introduction

Graphene, the super carbon , is now accepted as wonder material with new physics and it has caused major breakthrough in nanotechnology[1-3]. Graphene has been the main candidate for applications in semiconductor electronics and in other related fields [4-7]. After a decade of the discovery of graphene [7] , one may have to answer the following questions. Are the key technological huddles overcome successfully to realise the full applications of graphene? What is the current status of the graphene based devices or Electronics ? How the graphene market business is going to evolve in the coming years? What kind of graphene based products can one expect in the near future?. The main challenge in graphene is the opening of the band gap in the semimetallic electronic structure. In the bandstructure of graphene which is dominated by Dirac description, valence and conduction bands cross the Fermi level at a single point (K points) in the Brillouin zone and hence it is a is a zero gap semiconductor or a semimetal with zero density of states . Due to the linear dispersion of energy bands and appearance of Dirac cones near the 'K' point and Fermi level the electrons behave like massless Dirac fermions [1]. For applications in nanoelectronic devices a suitable band gap is essential. Opening a suitable bandgap in graphene will allow it to be used in the semiconductor industry for the fabrication of new 2-dimensional nanoelectronic devices such as solar cells, liquid crystal devices, and nanosized transistor prototypes [8].

There are various ways of manipulating the band structure and hence band gap in graphene. Several methods, for band gap engineering in graphene and similar materials, are suggested in the literature [9-30]. There is a large amount of work on vacancy defects in graphene [13-15,18-20,24] systems and a reasonable amount of theoretical work [19,21-24] are reported on substitutional covalent bonding in carbon/nitrogen, carbon/boron, and carbon/boron/nitrogen systems. Some of the extrinsic sources of manipulation are adatoms (functionalization), charges on top of graphene etc. In the literature [15-20] , several methods on structural and band gap modulations in graphene are available. Among them, the band gap opening through functionalization is widely reported [11,15-17,19]. Because of the sp2 bonding and robustness of graphene , it is very hard for the foreign atoms to replace the carbon atoms or get adsorbed. Moreover the adsorption mechanism depends on the chemical nature of the species. Doping could block interband transitions in single-layer graphene. However the surface doping (physisorbed adsorbates) of graphene may lead to a different situation. Also it has the advantage that it is technically feasible. we have also studied the band gap opening in graphene through application of external stress.

Manipulation of band gap in nanostructures is entirely different from that of the bulk materials. Even a little perturbation to a low-dimensional system will produce prominent changes in the structure and in turn in the electronic structure of the system. Being a nanostructured 2D crystal, graphene uniquely responds to the disturbances that are induced externally. The substitutional doping results in enhanced chemical reactivity of defective graphene. We,in this first principle study, considered band gap opening and modulation in graphene by i) Mono and di-vacancies; ii)Substitutional doping; iii)Functionalization with oxygen like atoms; iv) Induced Strain using density functional theory calculations.

Calculational methods

The calculations are carried out using DFT implemented plane wave code, Vienna ab-initio simulation package (VASP) [22]. The generalized gradient approximation with PW 91 functional [23] and projector augmented wave (PAW) potentials are used in the calculation. To simulate graphene, We have taken a slab of 24 carbon (C) atoms in a super cell of size, a = 8.52 Å, b = 7.378 Å and $\alpha = \beta = \gamma = 90^{o}$. In a certain study, we repeated the calculations for 96 atom system. A vacuum space of 11 Å is introduced between the periodic images of graphene sheets along the z-axis such that the interaction between them is negligible. The gamma centered 10×10×1 k-point grid is used in structural relaxations. The k-point grid is made denser with 50×50×1 k-points for accurate DOS analysis with the smearing width of 0.1 eV and band structure calculations. The geometrical structures are fully relaxed without any constraints using conjugate gradient algorithm. The convergence criterion is set as 1×10^{-6} eV between two ionic steps. The structures are relaxed until the force on each atom becomes 1×10^{-3} eV/Å.

Band gap opening and modulation in graphene with mono and di-vacancies(4) and Substitutional doping (1)

Results and Discussion

A. Vacancies in Graphene

We have examined the structural and band structure modification in graphene caused by the creation of single [28], double [28] and tri-vacancies (3 mono vacancies) in the basal plane. The missing of carbon atoms leads to vacancies in the plane of graphene layer. In our study, we have concentrated on single, double and tri-vacant sites in the graphene sheet. While mono and divacancies are investigated in a 24 atom slab and 96 atom slab of Graphene , the tri-vacancy and added impurities in them are investigated using 96 atom slab of graphene. The relaxed structures and charge distribution plots of graphene 24 atom slab and 96 atom slab are shown in Figs.1a,b,c & 1d. The band structures of planar graphene are shown in the Figs. 2a and 2b. The single vacancy is introduced with the removal of single carbon atom and the system is relaxed. In the relaxed structure, we can observe the existence of void space [Figs. 3a and 3b]. It leads to the conclusion that the vacant sites are not reconstructed and dangling bonds are present. There is buckling of carbon atoms that are present around the vacant site [Fig. 3c]. The charge distribution plot reflects the charge depletion region in the vacant site [Figs.3d, 3e, 3f & 3g] . The C–C bond lengths near the vacant sites decreased from 1.420 to 1.395 A°. The reduction in the C–C bond length confirms the presence of excess charge in those bonds [Figs. 3d and 3e-3g]. This is charge transfer of about 0.16 e to the carbon atoms surrounding the vacancy from the neighboring sites. As a result a small amount of electron charge is leaking into the vacancy site. This is clear from the charge distribution plot [Figs. 3d and 3e-3f]. Also, the out-of-plane movement of carbon atoms results in the structural distortion. In the band structure of graphene with single vacancy [Figs. 4a and 4b], we can observe the separation of the tips of the Dirac cones at the "K" point. The presence of topological defects affects the electron-hole symmetry of the two Dirac cones (out of the 4 Dirac cones) and localized band states appear near the Fermi level. The linearly dispersing valence and conduction bands observed in pristine graphene (in the form of Dirac cones) are shifted away from the charge neutrality point. Non-dispersing flat bands and quardratically dispersing bands are introduced. The set of bands near the Fermi level arises due to the localization of charges around the vacancy site. They are responsible for the magnetism induced in the graphene with mono vacancy. In Fig. 4c (96 atom slab), one can see a electron band gap of ~ 1.0ev , with this band gap the graphene can be tailored for device applications.

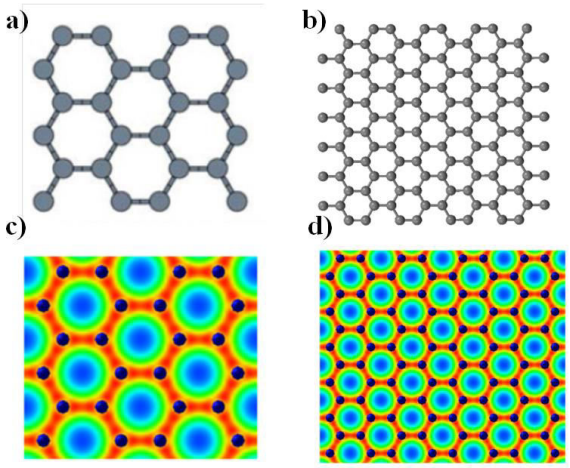

Figure 1. The relaxed structures of graphene slab a) with 24 and b) 96 carbon atoms. The charge distribution plots of graphene slab c) with 24 and d) 96 carbon atoms.

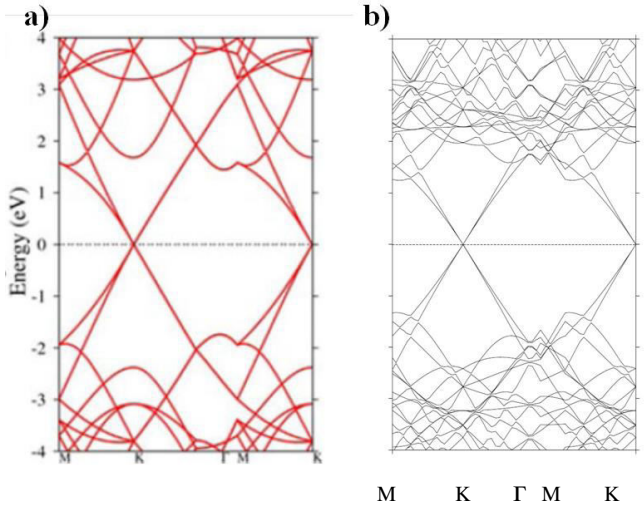

Figure 2. The band structures of a) 24 and b) 96 atoms graphene slabs.

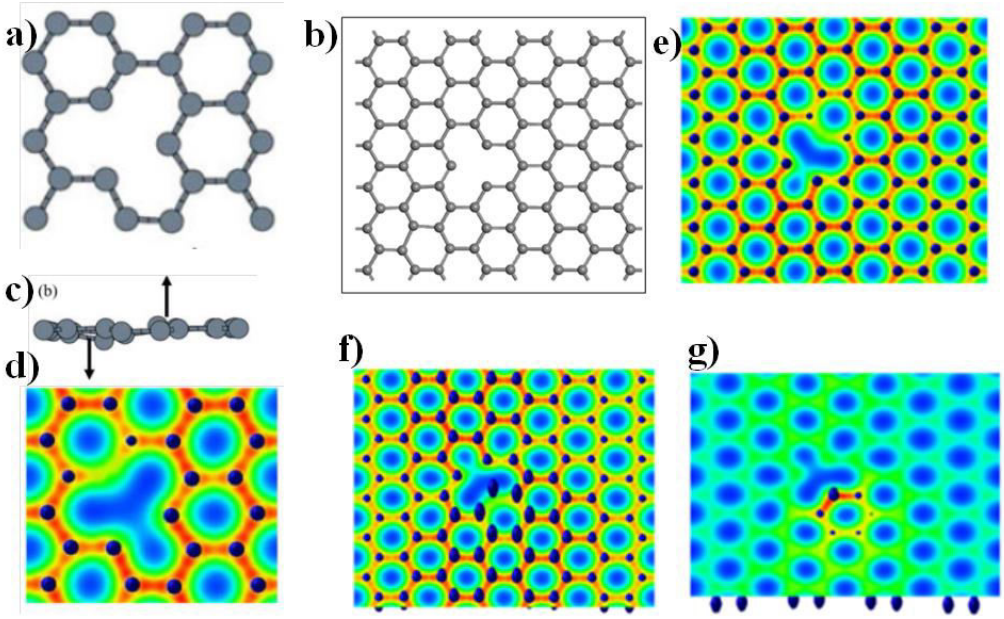

Figure 3. The relaxed structure of graphene slabs of a) 24 [28] and b) 96 carbon atoms with single vacancy. c) buckling of carbon atoms around the vacancy in 24 atoms graphene slab[28]. d) charge distribution plot of 24 atoms graphene slab with single vacancy[28]. e), f) and g) charge distribution plots of 96 atoms graphene slab with single vacancy.

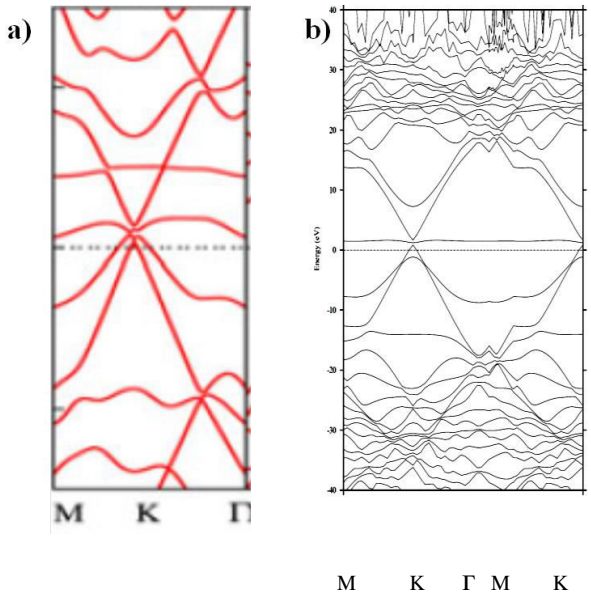

Figure 4. Band structures of graphene slabs of a) 24[28] and b) 96 carbon atoms with single vacancy.

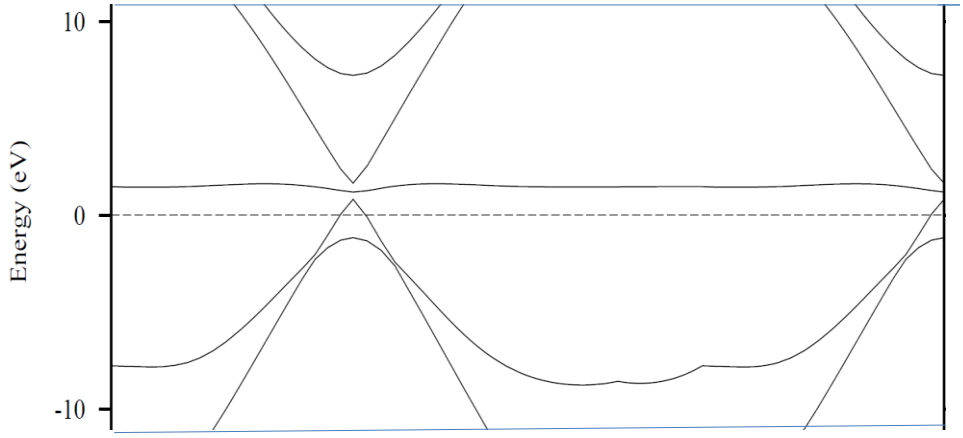

Fig.4c Closure view of the Bandstructure for G95+1Vac

The case of divacancy is different from that of the single vacant site [28]. There is no buckling of C atoms from the mean plane [Fig. 5a]. Instead, the C atoms around the divacancy have moved inward. The charge distribution plot clearly indicates the charge abundance around the vacancy site [Fig. 5b]. The C–C bond lengths in the armchair sites have decreased by 3.1%, whereas along zigzag sites the reduction is about 0.14% from original length. The charge depletion [see Fig. 5b] is reflected in the band structure. There is complete absence of flat bands near the Fermi level [Fig. 5c]. With divacancy , out of the two Dirac cones retained in the case of single vacancy , the upper cone moves further up above the Fermi level resulting in a larger band gap. The parabolic bands resulting from the other two Dirac cones move well above and below the Dirac cones. The lower cone retains its linear dispersion character but the upper Dirac cone looses 50% of its linear dispersion character.

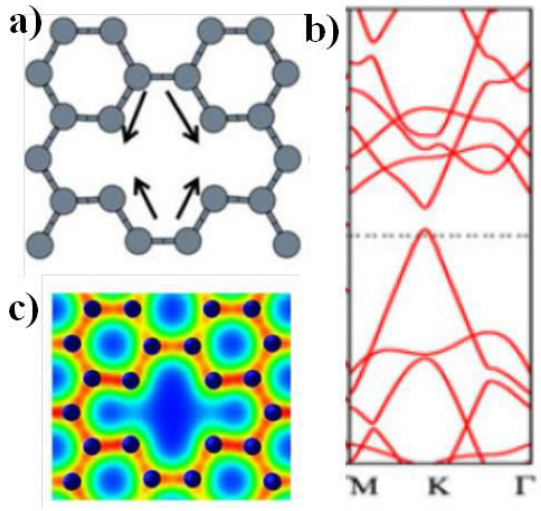

Figure 5. Divacancy in 24 atom graphen slab [28]. a) relaxed structure, b)band structure and c) charge distribution plot.

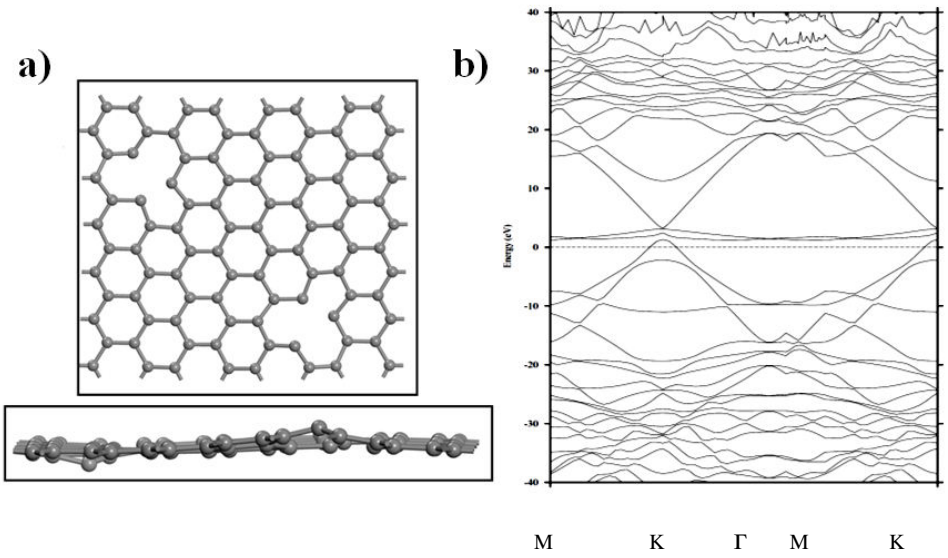

Figure 6. Two single vacancies in 96 atom graphene slab a) relaxed structure, and b) band structure.

In another case we have investigated the graphene system with two mono-vacancies (G94+2Vac). The relaxed structure and the corresponding bandstructure are given in Figs. 6a and 6b respectively. There is buckling (protrusion and depression) of carbon atoms that are present around the vacant site [Fig. 6a]. The doubly degenerate cone shaped bands are pulled apart leading to the opening of a different type of gap. Out of the four Dirac cones pulled apart, two of them retain their shape and stop moving further apart after the gap opening. The other two cone shaped bands loose their shape and become parabolic. Two flat bands due to localized charge states of the vacancy lie in the band gap between the separated tips (one V shaped tip and another rounded tip) of Dirac cones parallel to the FL and extends on either side of the cones (Fig. 6b). Effectively there is an in direct band gap (pseudo gap) of ~ 1eV. The shape of the Dirac cone below the FL is almost retained except its rounded tip. This semiconducting graphene with two monovacancies is better than the ordinary semiconductor because of the presence of Dirac cones and massless Dirac Fermions.

B. Impurity atoms in the vacancy

The charge accumulation and distortion will make the vacant site as preferential site for adsorption of foreign molecules. The vacant sites are like trapping centers such that they have a high tendency to adsorb the atoms/molecules such that graphene gets reconstructed. In order to further improve the band gap opening in the graphene we introduced impurity atoms in the vacancies and investigated the changes

in the bandstructure, mainly the band gap opening.

Hydrogen in the vacancies

First we created three mono vacancies in the 96 atoms slab of graphene and relaxed it. Then we introduced Hydrogen atoms one by one. The three relaxed structures and the corresponding bandstructures are given in Figs. 7, 8, and 9.The first relaxed structure with one hydrogen atom in one vacancy is given in Figs. 7a. The hydrogen atom in the vacancy is projecting out [Fig. 7a] of the plane while in other vacancy sites there is buckling of carbon atoms. We come across some interesting features in the band structure of graphene [Fig.7b] The charge distribution plot for this structure is depicted in Fig.7c. Two Dirac cones are shifted up above the Fermi level and a small gap opens up [Fig.7b] . In the gap lies one of the four Dirac cones now turned into a quadratically dispersing parabolic band. Similar thing happens to one of the upper Dirac cones. The hydrogen bands mixes with the graphene bands near the bottom of the inverted V Dirac cone and lie across the lower cones parallel but bellow the Fermi level and extends on either side of the cones. Apparently there is no band gap opening near the Fermi level, however well above the Fermi level, as mentioned there is a small gap. To make use of this gap we have to tune the system so that the gap moves closure to the Fermi level. We introduced one more hydrogen atom in one of the remaining mono-vacancies.

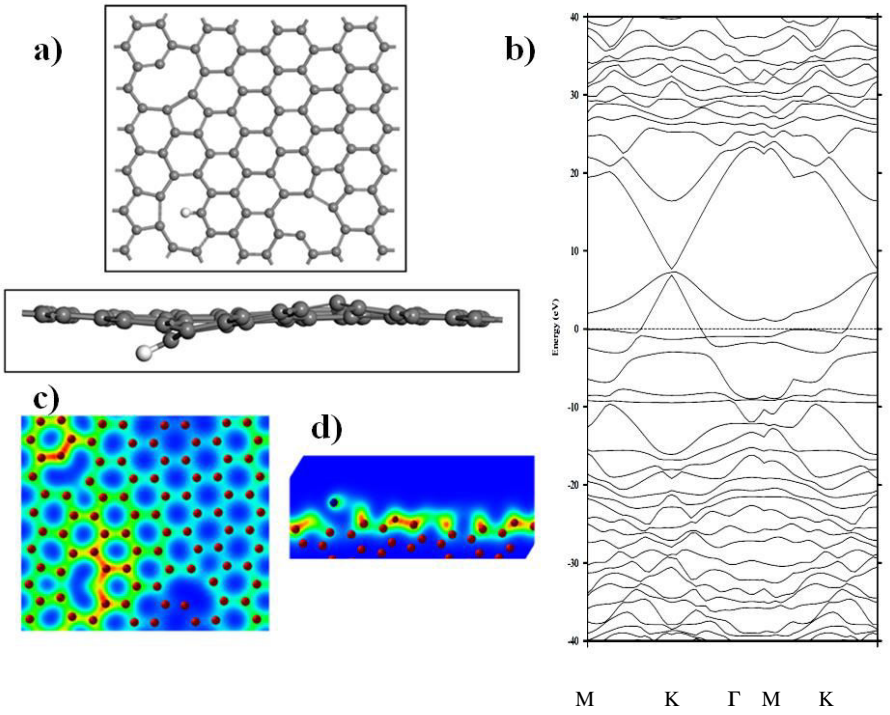

Figure 7. One H and two vacant sites in trivacant 96 atom graphene slab. a) relaxed structure, b) band structure and charge distribution plots with c) top view and d) side view.

The relaxed structure of graphene with two hydrogen atoms in the mono vacancies and the third vacancy is shown in Figs. 8a and 8b. The hydrogen atoms in the vacancies are projecting out [Fig. 8a] of the plane and there is buckling of carbon atoms. The corresponding bandstructure is given in Fig. 8b. The Dirac cones and the gap have moved down towards the FL , but not much. The bandstructure looks similar to the previous one [Fig.7b]. To get further movement of the gap we added the third hydrogen atom in the last monovacancy. The relaxed structurewith three hydrogen atoms in the mono vacancies is shown Fig. 9a. The hydrogen atoms in the vacancies are projecting out [Fig. 9a] of the plane and there is buckling of carbon atoms around the hydrogen atoms. The corresponding bandstructure is given in Fig. 9b. Now the Dirac cones and the gap have moved up away from the FL. The bandstructure looks similar to the previous ones [Figs. 7b and 8b].

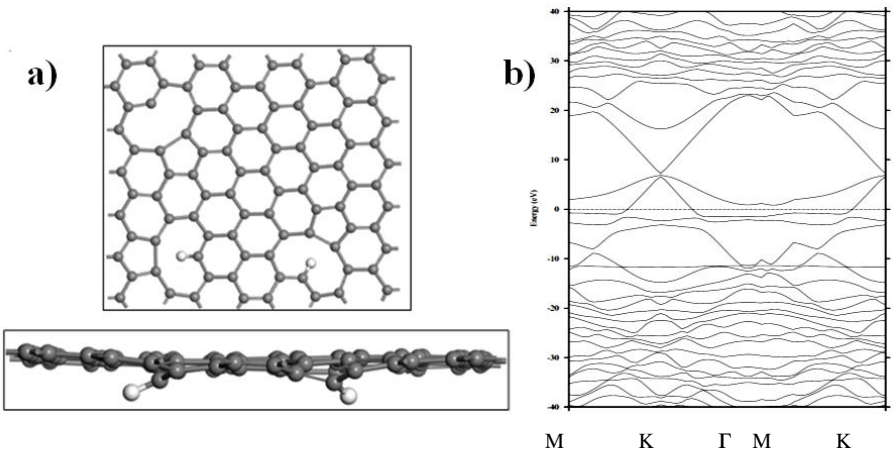

Figure 8. Two H and one vacant site in trivacant 96 atom graphene slab. a) relaxed structure, b) band structure.

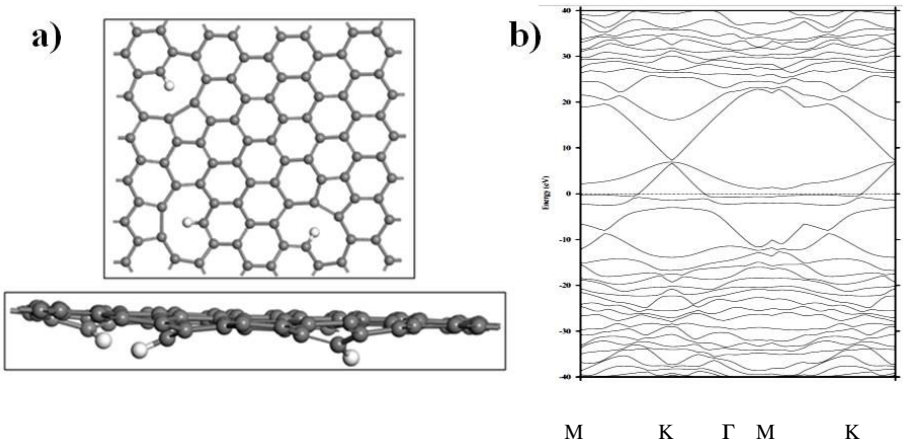

Figure 9. Three H in trivacant 96 atom graphene slab. a) relaxed structure, b) band structure

To summarize, tuning the band gap with multiple mono vacancies and gradual filling them with hydrogen atoms has not given the desired result. May be the interaction of hydrogen with the graphene is strong enough to spilt the Dirac cones and move them above the FL.

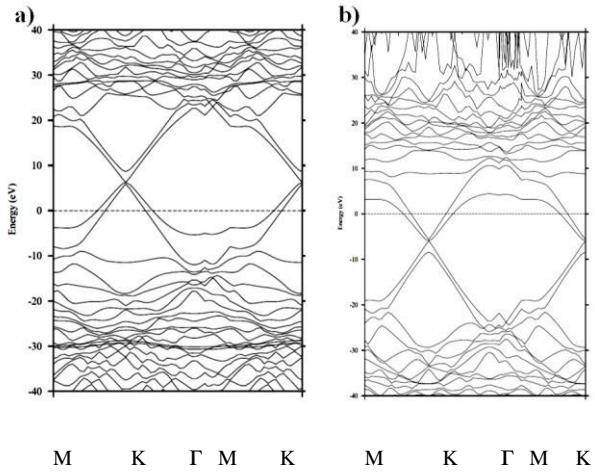

Figure 10. Band structures of a) boron and b) nitrogen doped graphene slab of 95 carbon atoms.

C. Substitutional doping in graphene

On substitution of boron (B) and nitrogen (N) atoms, E_F is shifted in opposite directions in the band diagram (Figs. 10a and 10b). The acceptor and donor bands are formed below and above EF in B-doped and N-doped graphene and obtain p-type and n-type graphene with B and N doping respectively. Both B and N are non-metals and they form covalent bonds with carbon atoms of graphene. Even after the substitution, the structure of graphene is maintained and there are no distortions except the change in inter-atomic bond lengths. The formation energy of boron doping is more than that of N atom. Therefore doping of graphene by N is thermodynamically favorable. In this case there is no band gap opening, only bands shifting , for the doping of N and B individually [29].

We then tried co-substitution. The co-substitution of B and N leads to equal concentrations of p-type and n-type impurities and the degenerate bands get splitted and move symmetrically above and below Fermi level. Here also no band gap opens.The co-substitution of B and N is interesting. The conduction and valence bands cross the Fermi level at the 'K' point. But the bands are not perfectly linear and the Dirac cones are distorted. The touching of the distorted Dirac cones at the Fermi point can be a check mark for presence of equal concentration of p-type and n-type impurities in graphene. The degenerate bands are split . This is due to B and N atoms and the strain in the inter-atomic bonds induced by the substitution. The carbon atoms acquire electrons from B and lose electrons to N. Accordingly the degenerate bands get splited and move symmetrically above and below Fermi level. The individual N atoms displace the C atoms from the graphene lattice and half of the extra electronic charge obtained through N doping is distributed throughout graphene lattice while the remainder is localized around the N atoms. This is the mechanism of complementary doping applied to graphene [29].

In the case of co-substitution of B and N, a third suitable dopant element which will upon substitution induce a small gap, has to be identified. In this process the percentage of N and B is increased to check the effect on band gap. The systems investigated are (G93+NBB) and (G93+BNN). The relaxed structures and the corresponding electronic bandstructures are shown in Figs. 11 and 12. Since the B-N pairs are isoelectronic to C-C pairs in the relaxed structures there are no buckling or any other distortions. In the bandstructure also we did not get any major changes . The bandstructure of (G93+NBB) [Fig. 11b] looks similar to the B doped graphene bandstructure [Fig. 10a] and (G93+ BNN) bandstructure [Fig. 12b] mimics the N doped graphene bandstructure [Fig.10b].

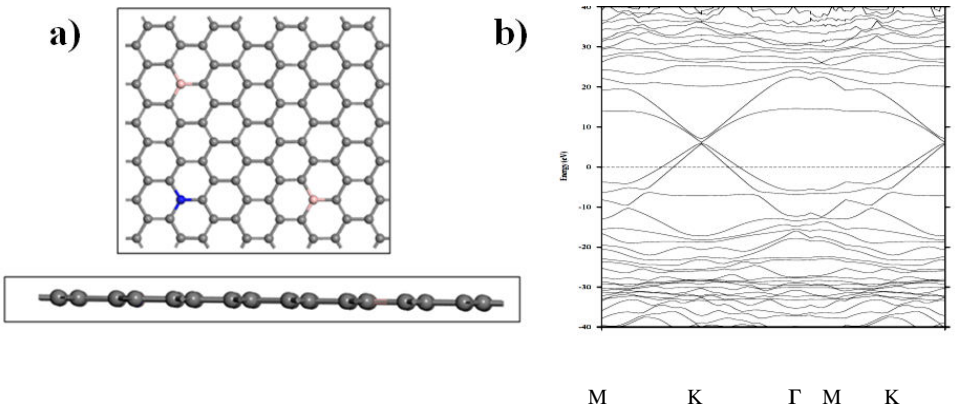

Figure 11. a) relaxed structure and b) band structure for G93+NBB.

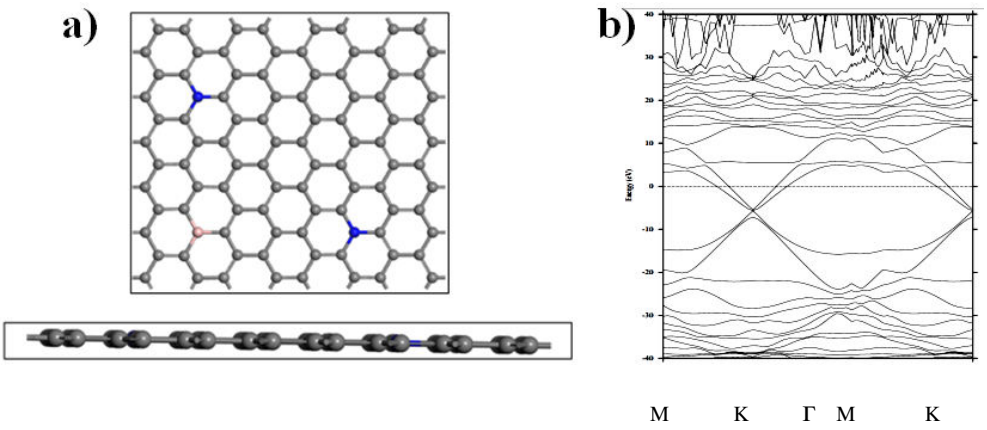

Figure 12. a) relaxed structure and b) band structure G93+BNN.

In the above tri-doping , we wanted to change the third dopant so that it will lead to band gap opening in graphene. From our experience in band gap engineering using surface doping of various atoms we could reason out that the third dopant could be sulphur (S) only. In the above systems ,(G93+NBB) and (G93+BNN) , we replaced the second B/N by S . The relaxed structure (G93+BNS) is shown in Fig. 13a. The corresponding bandstructure and charge distribution are given in Figs. 13b and 13c, respectively. If one examines the relaxed structure , it is clear that sulphur has interacted strongly with graphene and it has caused buckling in the structure around it. The S is projecting out of the graphene plane. This interaction of S with graphene has altered the electronic bandstructure of (G93+NBB) / (G93+BNN). The doubly degenerate cone shaped bands are pulled apart leading to the opening of gap. Out of the four Dirac cones pulled apart, two of them retain their shape and stop moving further apart after the gap opening. The other two cone shaped bands loose their shape and mixes with the sulphur bands and lie in the band gap between the rounded tips of the less distorted Dirac cones parallel to the FL and extends on either side of the cones. Effectively there is a direct gap of ~ 1eV and the shape of the Dirac cone below the FL is almost retained except its rounded tip. As a result the graphene substitutionally co-doped with S has turned into a semiconductor with massless Dirac fermions and electrons contributing to its carrier mobility. This graphene semiconductor is better than the ordinary semiconductor because of the presence of Dirac cones and massless Dirac Fermions. This will have lot of application in device industry compared to a pristine graphene because of the presence of a gap and Dirac cones.

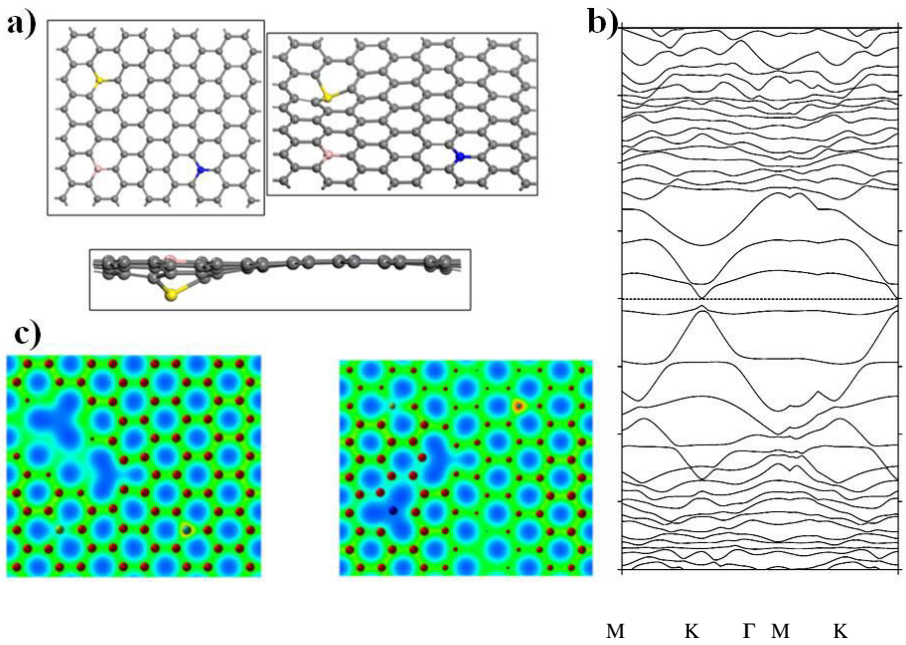

Figure 13. a) relaxed structure, b) band structure and c) charge distribution plots for G93+BNS.

To get band gap opening in graphene through substitutional doping, we stated with B and N and increased their percentage. Finally S is co-doped along with B and N. This substitutional co-doping leads to a direct band gap opening in graphene retaining major linear portions in one of the Dirac cones. Direct single substitutional doping with S would have distorted (protrusion and depression of C atoms) the graphene to a larger extend leading to the destruction of linearity of all the Dirac cones, that is why we tried co-substitutional doping of S. The band gap can be experimentally tuned by altering the doping parameters doping energy and concentration [33].

Functionalization with oxygen like atoms (2)

In this part of investigation, we have tried surface doping for modifying the electronic structure of graphene. The surface doped atoms are physisorped. In a previous calculation [28], we have functionalized graphene with oxygen atoms with different coverages and have demonstrated the change in the structural and electronic properties of graphene. For a single O atom a gap of 0.08eV opens up and the Dirac cones made of single bands separated at their tips appear. For more number of surface doped O atoms the gap is large and the Dirac cones are completely destroyed. Taking this as a clue we have surface doped graphene with 'Oxygen like atoms' and looked at the band structure. Such studies are not available in earlier reports involving above investigations and in some of the available works, theoretical methods other than first principles density functional theory (DFT) are employed. In this work we have used first principles calculations based on DFT and we have come up with the results obtained from binding energy, band structure and DOS calculations. We have got some interesting results that have not been reported earlier.

It is known[29] that substitutional doping of graphene leads to n-type or p-type graphene depending upon the the dopents also doping could block interband transitions in single-layer graphene . It was reported[11] that it is technically feasible to modify the bandstructure of graphene by physisorbed adsorbates . As pointed out by Kozlov et al [11] this process has advantage of flexibility in realizing the surface adsorbed layer. By surface doping the band gap engineering can be controlled in different ways. As pointed out in the previous section ,for the surface doping of graphene with oxygen atom, band gap opening is observed. But the band gap was very small and the Dirac cones are retained to some extend. In order to increase the band gap and at the same time retain the Dirac cones, which is the manifestation of massless Dirac fermions, We have surface doped graphene with oxygen like atoms F,P,Cl & S and B,N atoms isoelectronic to carbon atom and molecules SO_2,CO_2, N_2 & BH_3.

Results and discussion

D. Graphene surface doped with oxygen like atoms

The relaxed structure of graphene (G24) is shown is Fig. 1a. The band structure of this planar graph1ene is shown in the Fig. 1b. The presence of delocalized π electrons is obvious from the charge distribution plot (Fig. 1c). The relaxed structure of 96-atom slab graphene (G96), its bandstructure and charge distribution are given in Fig.2. The results, the relaxed structures and the corresponding bandstructures of the surface doping of graphene with oxygen like atoms F,Cl,P & S are given in Figs. 3, 4, 5 and 6 respectively. Out of the surface doped cases, the surface doping with Sulfur (S) atom alone leads to gap opening in the bandstructure of graphene.

The relaxed structure and bandstructure of G24 surface doped with Flurine (F) look like the one given in Fig.3a & b The energy degeneracy of the Dirac cone bands is removed and the outer Dirac cones retain the cone shape the inner cones are distorted. The two Dirac cones are shifted up above the Fermi level and a small gap opens up. The flurine band lies in the gap and extends on either side of the cones.

The bandstructure of graphene (G24) doped with Cl is given in Fig.4b. No gap opens up , the Dirac cones are shifted up above the Fermi level through 10.0eV. The Cl bands mixe with the graphene bands near the Dirac cones, as a result there is discontinuity in the lower portion of the lower Dirac cone. The Cl bands lie across the lower cones parallel to the fermil evel and extends on either side of the cones.

The relaxed structure of G24 surface doped with P is given in Fig.5a. The corresponding bandstructure with a large gap is shown in Fig.5b. The doubly degenerate cone shaped bands are pulled apart leading to the opening of gap. Out of the four Dirac cones pulled apart, three of them retain their shape but with rounded off tips. The P bands lie in the gap near the Fermi Level (FL). But for the presence of the P bands in the gap near the FL, G24 surface doped with P would have qualified as a good semiconductor.

The relaxed structure of G24 surface doped with S is given in Fig. 6a and the corresponding bandstructure is depicted in Fig. 6b. Due to the surface doping a direct band gap of 1.4eV opens up at the K-point. The density of states plot (Fig. 6c) also has the signature for gap opening. The band gap arises due to the interaction of p electrons of S with the pz electrons of graphene. This is evident from the charge distribution plot (Fig. 6d). As a result the doubly degenerate cone shaped bands are pulled apart leading to the opening of gap. Out of the four Dirac cones pulled apart, two of them retain their shape and stop moving further apart after the gap opening.

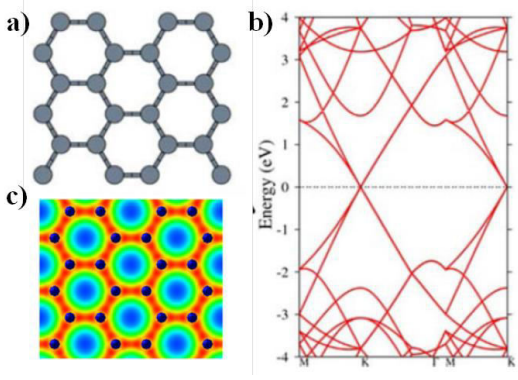

Figure 1. a) relaxed structure, b) band structure, and c) charge distribution plot for graphene (G24)

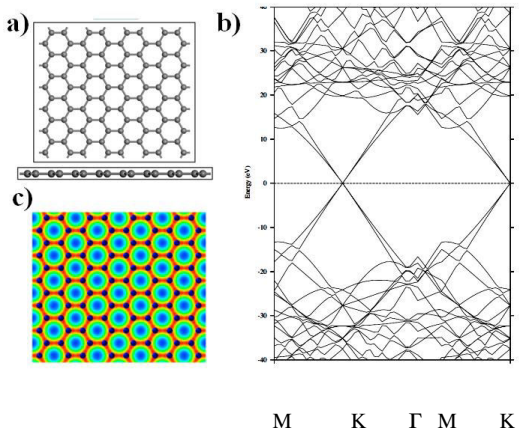

Figure 2. a) relaxed structure, b) band structure, and c) charge distribution plot for graphene (G96)

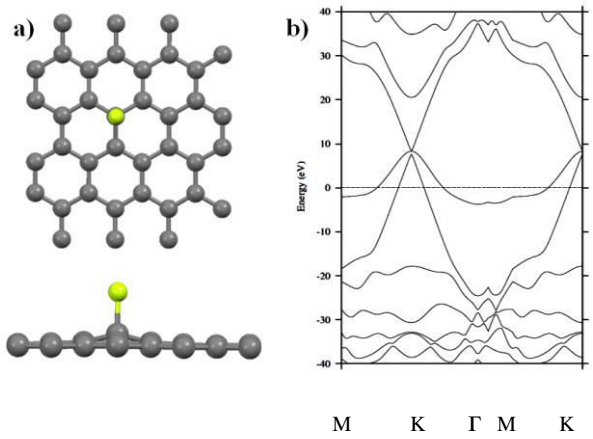

Figure 3. a) relaxed structure, and b) band structure for G24+F

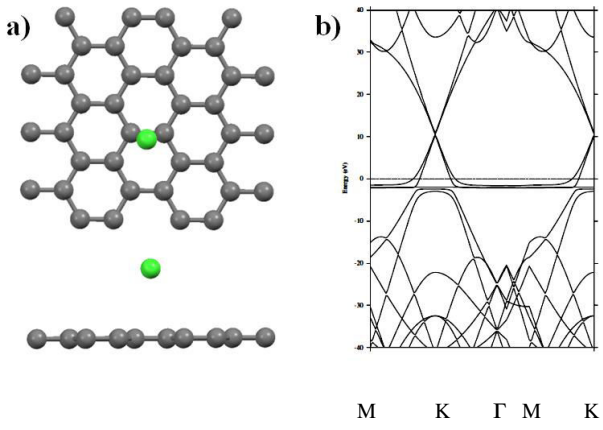

Figure 4. a) relaxed structure, and b) band structure for G24+Cl

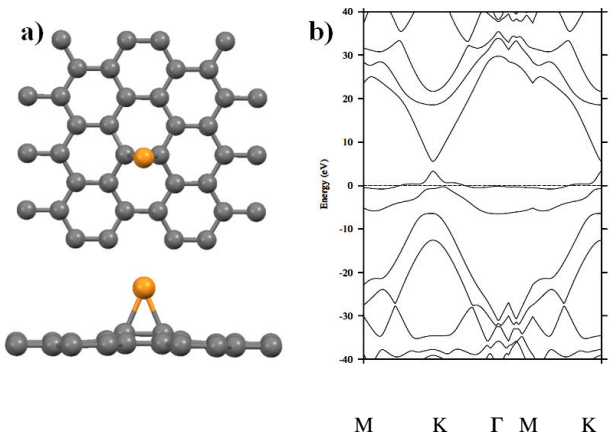

Figure 5 a) relaxed structure, and b) band structure , for G24+P

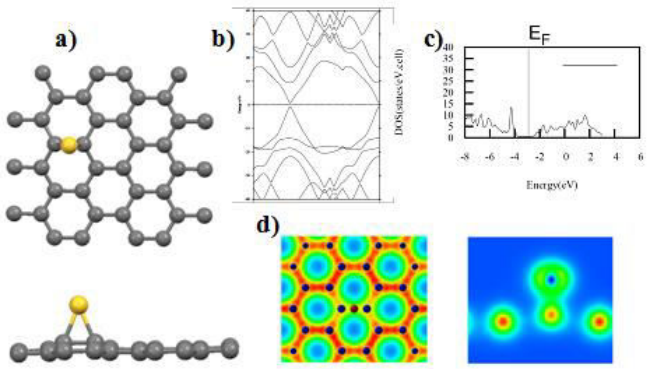

Figure 6 G24+S: a) relaxed structure, b) band structure, c) density of states, and (d) charge distribution plots with top and side views

The other two cone shaped bands loose their shape and become parabolic in shape and move away (below and away) further from the the cone tips. Finally the graphene surface doped with S is a semiconductor with massless Dirac fermions and electrons contributing to its carrier mobility. A closure view of the bandstructure near the gap is presented in Fig.6e.

Similar situation arises when we repeated the calculations with G96 as shown in (Fig.7). To fine tune the band gap we fixed the distance of Sulphur atom and got the relaxed structures and the band structures (Figs. 8a and 8b). The change in the distance of S from G96 is too low that there is hardly any change in the band gap. For G96+S the band gap is around 1.0eV and the Dirac cones are in better shape than the case with G24. A closure view of the bandstructure near the gap is presented in Fig.8c.

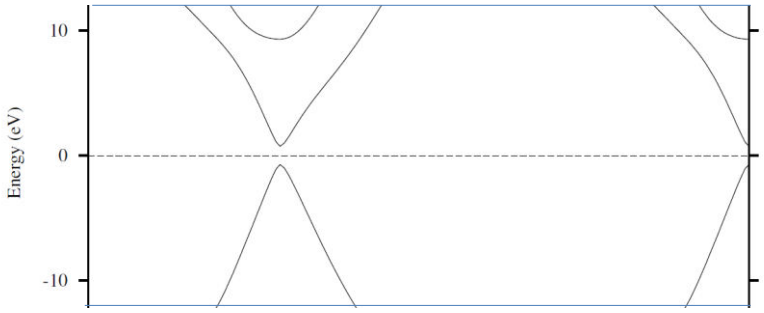

Fig.6e Closure view of the band gap for G24+S

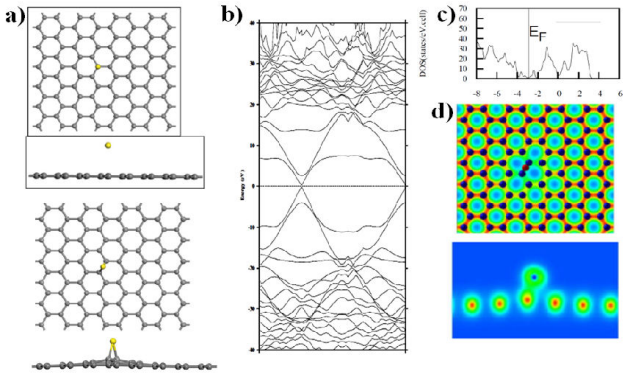

Figure 7. G96+S: a) relaxed structure, b) band structure, c) density of states, and (d) charge distribution plots with top and side views.

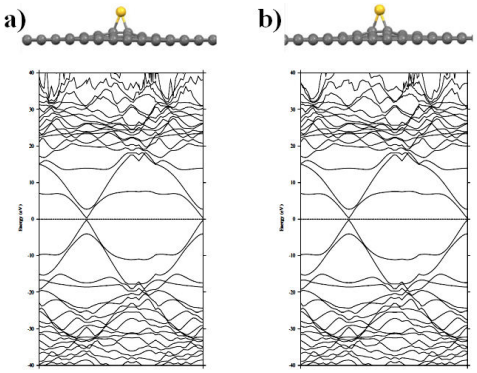

Figure 8 Relaxed and band structures of G96 with: a) free S, and b) fixed S.

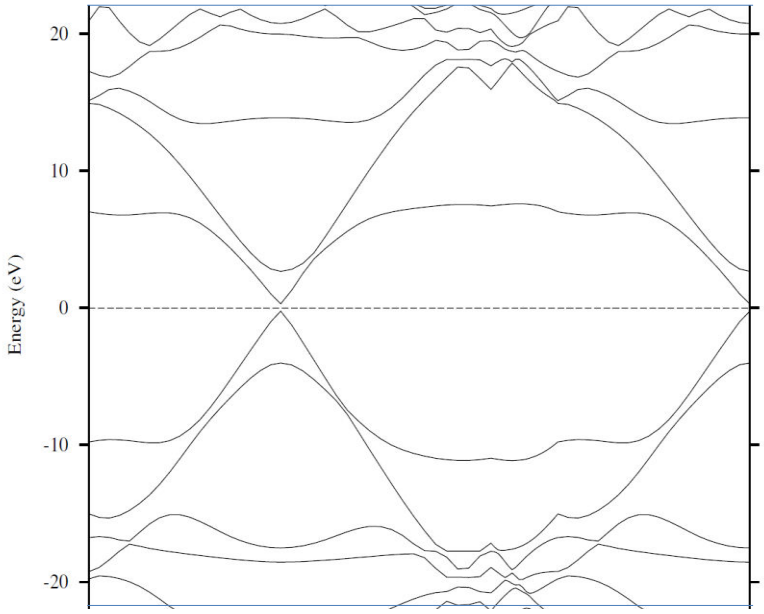

Fig. 8c Closure view of the Bandstructure near the band gap for G96+S

This graphene semiconductor is better than the ordinary semiconductor because of the presence of Dirac cones and massless Dirac Fermions. This will have lot of application in device industry compared to a pristine graphene because of the presence of a gap and Dirac cones.

B.Tuning the band gap

Next we tried to modify the surface doping so that we will have control over the band gap. We changed the position of the surface doped S atom and relaxed the structure (Fig. 9a). The band structure corresponding to this is shown in Fig. 9b. There is no change in the bandstructure, with the surface doping of single S atom the bandstructure is sensitive to the distance between S and the surface of grapheme not on the position of the S atom. Then we increased the number of surface doped sulphur atom. We surface doped with two S sulphur atoms. For one orientation (Fig.10a) of the two sulphur atoms a large gap (12eV) opens up in the graphene bandstructure (Fig.10b). The bandstructure is completely modified. The Dirac cones disappear, and doped graphene looses all its special features. For the other orientation (Fig. 11a) of the two sulphur atoms , the bandstructure of doped graphene looks like the one given in Fig. 11b. No gap opens up , the Dirac cones are shifted up above the Fermi level through 5.0eV. The sulphur bands mixes with the graphene bands near the Dirac cones, as a result there is discontinuity in the lower portion of the lower Dirac cone. The sulphur bands lie across the lower cones parallel to the fermilevel and extends on either side of the cones. The two sulphur atoms are at a distance of 3.94A from G24 and the planar nature of graphene is not disturbed and as a result there is no band gap opening, only shifting of bands (Fig.11b). We surface doped two S atoms on G96 for two different distances between the two S atoms. In the relaxed structures (Figs. 12a and 12b) the two S atoms are at distances 1.921Å and 1.946Å from G96. Here also the planar nature of G96 is not disturbed, that means no band gap opening will occur for surface doping of two S atoms.

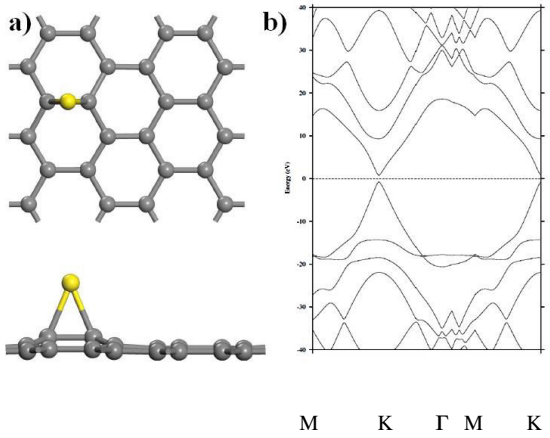

Figure 9. G24+S in different position: a) relaxed structure, and b) band structure.

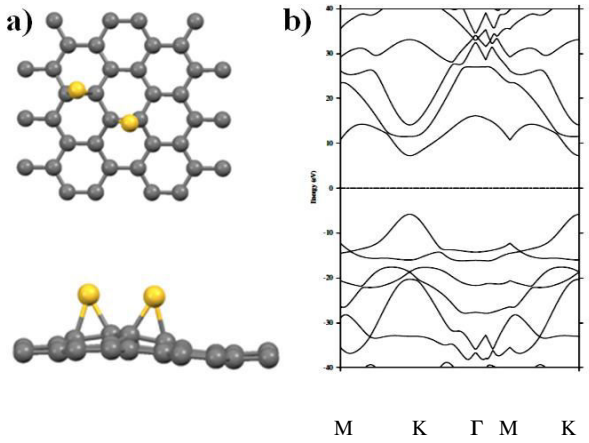

Figure 10. G24+2S: a) relaxed structure, and b) band structure.

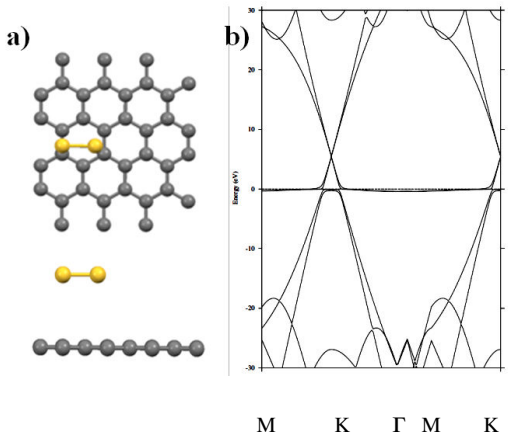

Figure 11. G24+2S in different position: a) relaxed structure, and b) band structure.

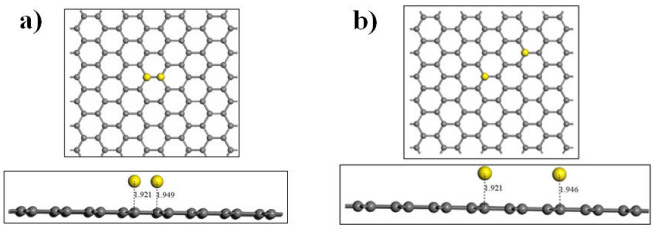

Figure 12. a) and b) the relaxed structure of G96+2S in different positions.

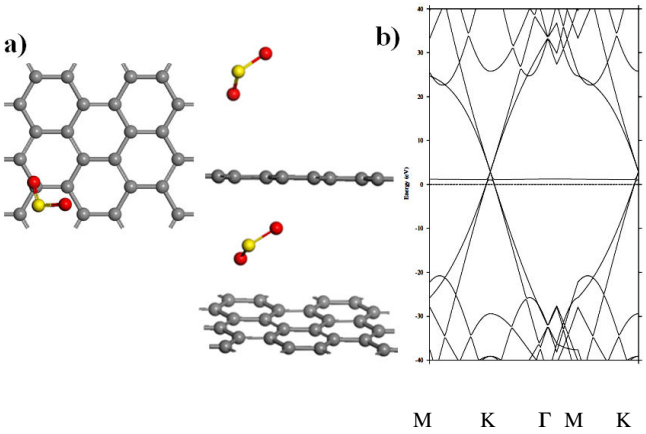

Figure 13. a) relaxed structure, and b) band structure for G24+SO_2

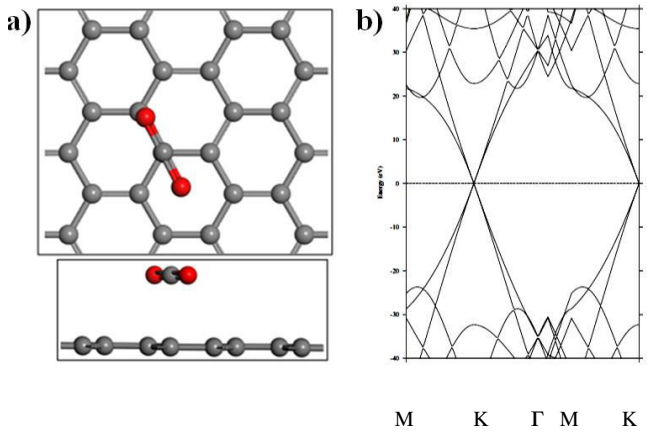

Figure 14. a) relaxed structure, and b) band structure G24+CO_2

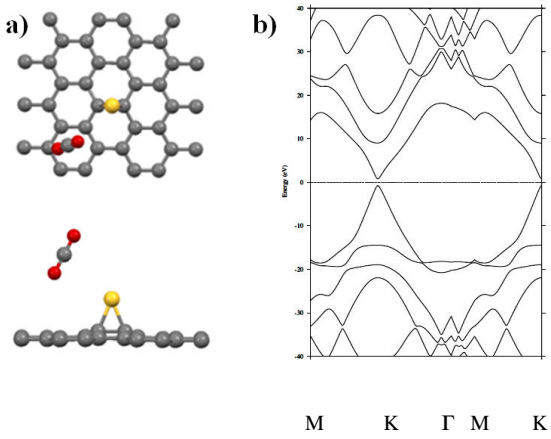

Figure 15.: a) relaxed structure, and b) band structure for G24+ CO_2 +S

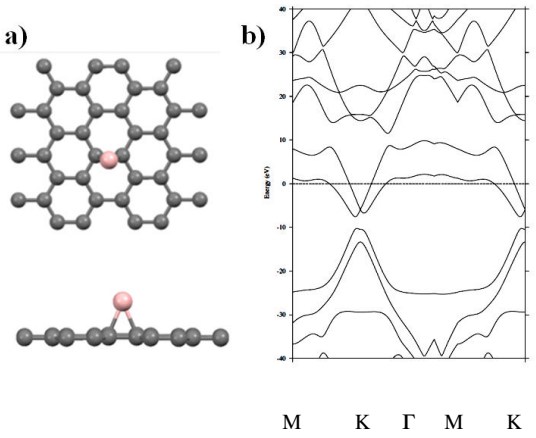

Figure 16. a) relaxed structure, and b) band structure for G24+B

C. Co-doping

To further improve and control band gap opening through surface doping using sulphur as the surface dopent , we added a co-dopant along with S. Since we have already effected band gap opening, retaining Dirac cones, using O and S separately, we tried simultaneous surface doping of graphene with S and O. The best way, we thought, is surface dope graphene with SO_2. The relaxed structure is given in Fig. 13a. The corresponding bandstructure is given in Fig. 13b. Surprisingly the surface doping of graphene with SO_2 does not effect any band gap opening. The Dirac cones

intersection point is shifted slightly above the FL and there arises discontinuity in the lower Dirac cones (Fig. 13b).

Next we surface doped graphene with CO_2 and relaxed the structure which is given in Fig. 14a. The corresponding bandstructure is given in Fig.14b. This bandstructure looks exactly like the bandstructure of pristine graphene. Since the CO_2 molecule is a little far away from G24, neither C nor O atoms have any effect on graphene. Now we surface co-doped S along with CO_2. The relaxed structure is shown in Fig.15a, and the corresponding band structure is in Fig. 15b. The bandstructure looks similar to the bandstructure of graphene (G24) surface doped with S alone (Fig. 6a). Like in G24+S, here also a band gap of 1.4eV opens up, the two Dirac cones are retained with rounded off cone tips.

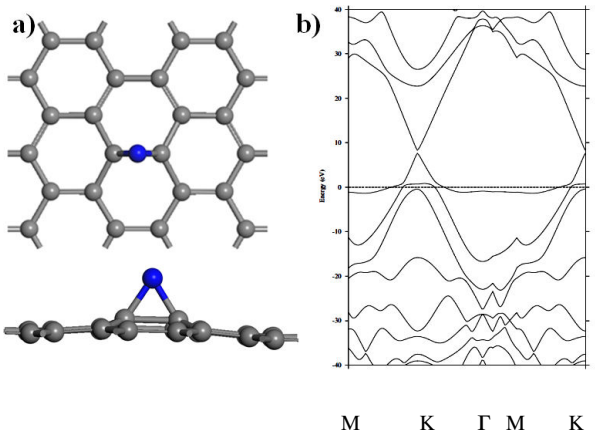

Figure 17. a) relaxed structure, and b) band structure for G24+N

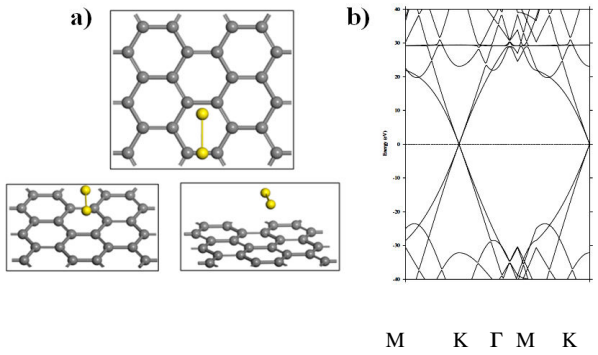

Figure 18. a) relaxed structure, and b) band structure for G24+NN

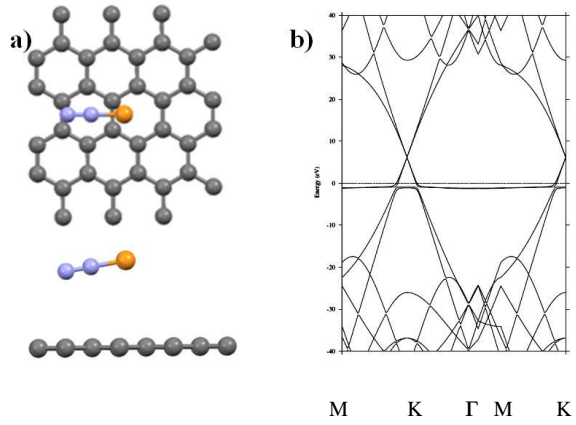

Figure 19. a) relaxed structure, and b) band structure for G24+NN +P

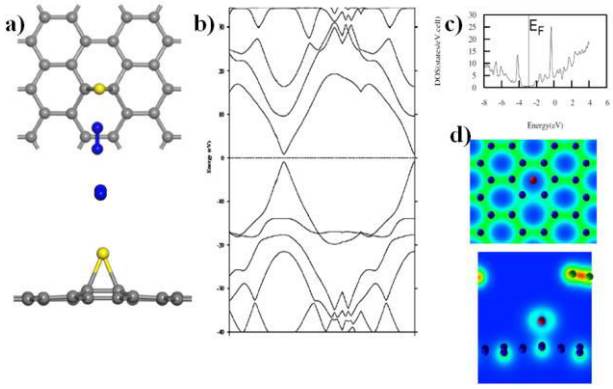

Figure 20. a) relaxed structure, and b) band structure for G24+ NN +S

We know [29] that when B is doped substitutionally in graphene ,it leads to p type graphene. No gap opens up. When we surface doped graphene (G24) with B (Fig. 16a), the two Dirac cones are shifted down below the Fermi level and a large gap opens up (Fig. 16b). The energy degeneracy of the Dirac cone bands is removed and the Dirac cone edges are rounded off and distorted. The upper Dirac cones have shifted latterly also. The boron bands mix with the graphene bands near the bottom of the Dirac cones.

It is also known that when N is doped substitutionally in graphene ,it leads to n type graphene. No gap opens up. When we surface doped graphene with N and NN , we come across some interesting features in the band structure of graphene. With a single N (Fig. 17a), the two Dirac cones are shifted up above the Fermi level and a small gap opens up (Fig. 17b). The nitrogen bands mixes with the graphene bands near the inverted V Dirac cones. The nitrogen bands lie across the lower cones parallel but bellow the fermi level and extends on either side of the cones. When one more N is added (Fig. 18a) , we get a band structure (Fig.18b) similar to a pristine graphene (Fig.1b). The nitrogen bands are well bellow and above the Dirac cones. Here we come across a different type of complimentary doping similar to the complementary substitutional doping of N and B in graphene. To engineer a band gap, along with NN we doped different elements like P ,S.

When P is added to G24-NN system (Fig.19a) the band structure is completely modified and looks as the one given in Fig.19b and similar to the bandstructure (Fig.17b) of G24+N system (Fig.17a). No gap opens up, the Dirac cones are shifted up above the Fermi level but without any distortion, the linearity of the bands is fully retained. The nitrogen and P bands mixes with the graphene bands near the Dirac cones, as a result there is discontinuity in the lower portion of the

lower Dirac cone. The N and P bands lie across the lower cones parallel and just bellow the fermi level and extends on either side of the lower cones.

When we surface doped S instead of P in G24-NN (Fig. 20a) , the bandstructure (Fig.20b) looks similar to the bandstucture of G24-S (Fig. 6b) or G24-CO2+S (Fig.15b), but now the

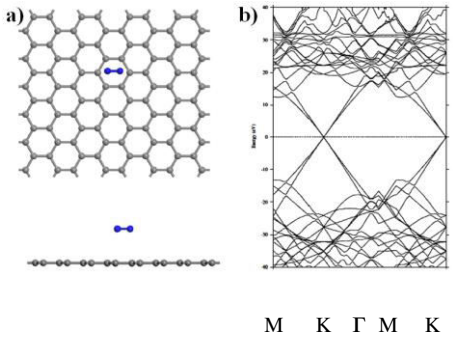

Figure 21. a) relaxed structure, and b) band structure for G96+NN

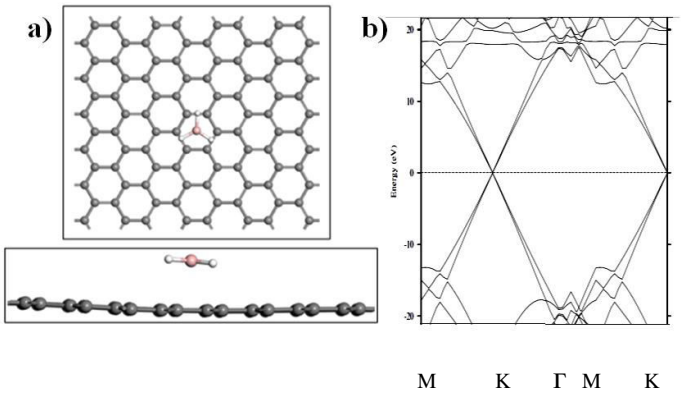

Figure 22. a) relaxed structure, and b) band structure for G96+BH_3 on C site

band gap value has increased to 1.5eV. It is reflected in the density of states (Fig.20c). The nitrogen atoms are at a distance of 5Å. And there is a very weak interaction between graphene and them where as S atom is at a distance of 1.92Å and a strong interaction is established between S and G24. This is clearly brought out in the charge distribution plot (Fig.20d).

We surface doped the graphene (G96) with diatomic molecule nitrogen (N2). The relaxed structure and the corresponding bandstructure are given in Figs. 21a and 21b respectively. We get a band structure (Fig. 21b) similar to a pristine graphene (Fig. 1b). The nitrogen bands are well bellow and above the Dirac cones. The present situation is similar to what we got for G24+NN (two nitrogen atoms well separated (Fig. 18a).

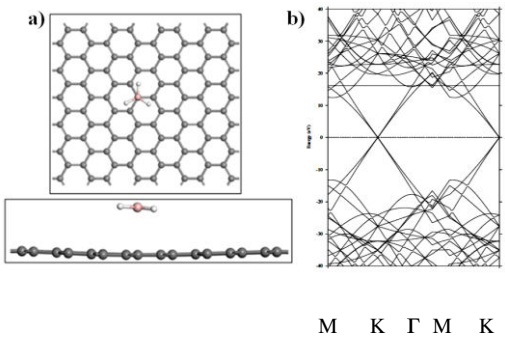

Figure 23. a) relaxed structure, and b) band structure for G96+BH_3 on hex site

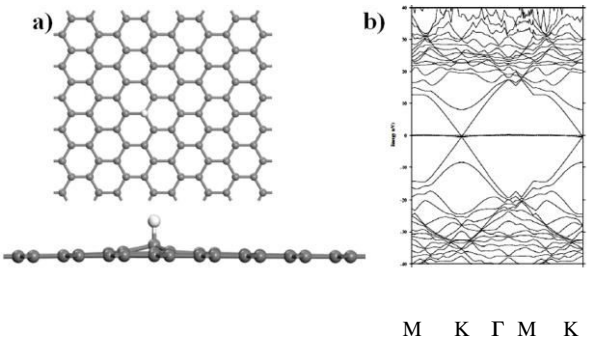

Figure 24. a) relaxed structure, and b) band structure for G96+H

We from our previous calculation [30] BH_3 molecule is found to be a good adsorbent on CNT and C60. In the same line graphene is surface doped with BH_3. There are two preferable sites on the graphene (G96). One is on C (Carbon) site and the other one is hexagonal site. The relaxed structures and the corresponding bandstructures for the adsorption of BH_3 on C site & hex. site are shown in Figs. 22 and 23 respectively. The bandstructures looks similar to the band structure of graphene (G96) (Fig. 2b). Even though the two bandstructures look alike without any gap, a closure inspection reveals that in the bandstructure (Fig.23b) corresponding to the hex. site the Dirac cones are getting separated and their degeneracy is being removed. Further suitable co-surface doping may lead to band gap opening.

Finally for comparison we surface doped graphene (96 atom slab) with hydrogen atom. The relaxed structure and the corresponding bandstructure are given in Figs. 24 and 24b respectively. H is bonded strongly with the graphene and the bonding site is very much distorted. In spite of its strong interaction there is no band gap opening. The flat hydrogen band lies parallel to the FL passing through intersecting point of the Dirac cones (Fig. 24b).

Concluding Remarks

Out of the different cases of surface doping of graphene with various atoms and molecules, the cases involving Sulphur turn out to be useful leading to band gap opening. Sulfur interaction with graphene surface is unique (see Table 1) . It moderately distorts the surface atoms and the interaction is limited such that a band gap opens without much distorting the Dirac cones. With single S a band gap of 1.4eV opens up. Also when S is co-doped along with CO_2 or with NN similar band gap opening occurs. But if it is co-doped with another S then the interaction is completely modified.The calculation of surface doping of graphene with S is repeated with 96 atom simulation cell. The band gap value is 0.7 eV. The value of band gap can be tuned to the required value by varying the distance of S atom from the surface of graphene, which can be achieved by proper ion implementation technique or by atomic layer deposition directly using remote oxygen plasma surface pretreatment [33]. The later technology is compatible with the traditional CMOS process which brings much possibility to future graphene devices [33].

Dopant	Distance (Å)	B. E. (eV)
O	1.50	4.07
S	1.94	1.76
S12	1.98	1.77
S12S22	2.00	1.79
SS	3.59	3.36
Si	2.05	1.22
Cl	2.86	1.08
F	1.84	2.42
P	2.03	1.62
N	1.45	5.19
B	1.67	1.25
S(NN)	3.84	2.82
Sfix(NN)	1.64	1.66
SS(NN)	3.65	3.33
S(CO2)	1.72	1.36

Table -1 Distances and Binding Energies of Surface Dopants

Strain-induced band gap opening in graphene(3)

Introduction

Based on first-principles study, we have investigated on the band gap opening in graphene through application of external stress. Our study suggests that this mechanism alter both structural and electronic properties of graphene. The combined action of structural modifications that involves stretching and compression of C–C bonds in the hexagonal network and charge localization mechanism are responsible for the gap opening in electronic spectrum of graphene, which is essential for the future application of graphene in electronics.

Simulation of strain in graphene

One can strain the graphene in three different ways. (i) The graphene sheet can be subjected to tensile stress in *x*-direction, (ii) It can be stained along *y*-direction, (iii) The graphene sheet can also be stained along both *x* and *y* directions. In order to introduce a strain of about 1.4% , a suitable stress is applied to the C–C bonds in the graphene lattice such that the C–C bond lengths increase to 1.44 from 1.42 A°. In the simulation cell C–C distance in the armchair bridge sites is selected as 1.44 A° and this configuration is equivalent to application of stress in the *x*-direction producing a stress of 1.4%. For *y*-direction, the zigzag C–C sites are stretched to the bond length, 1.44 A°. The application of stress along both x and y directions is effected by setting all C–C bonds equal to 1.44 A°.

Graphene under 1.4% strain

For the relaxed structure of graphene strained in *x* direction, we obtain the C–C bond lengths along *x*- and y-direction as 1.4375 and 1.4262 A,° respectively. For this case we get a band gap of 0.117 eV (Fig. 1a) . When the graphene sheet is subjected to a strain of 1.4% along the *y*-direction, the C–C bond lengths along *x*- and *y*-directions come out, after relaxation, as 1.4234 and 1.4387 A,° respectively. The highest occupied molecular orbital (HOMO) and lowest unoccupied molecular orbital (LUMO) get separated at the "K" point with a gap of 0.155 eV (Fig1b). Next graphene is subjected to biaxial stress (along *x*- and *y*-directions), in the relaxed structure the C–C bond lengths in the armchair bridge sites have bond lengths equal to 1.428 A°. The C–C bond lengths in the zigzag sites are equal to 1.448 A°. From this one can infer

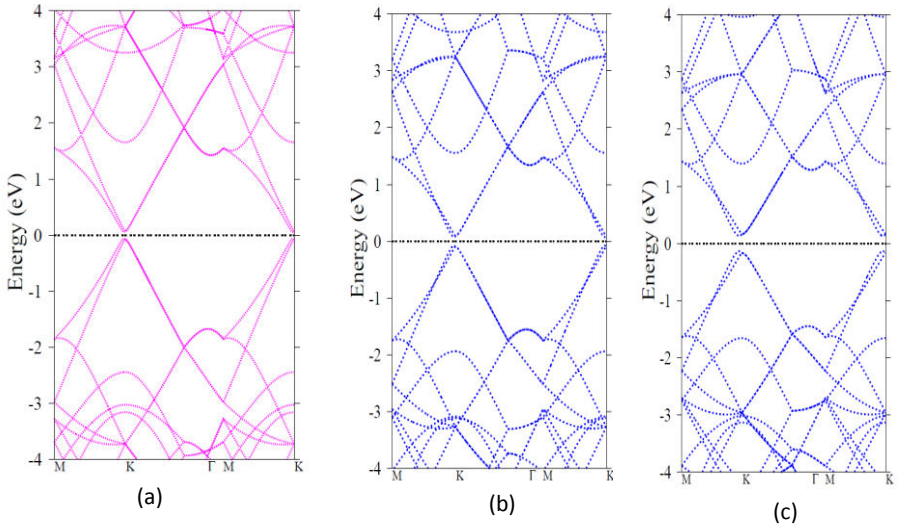

Fig. 1 Bandstructure of G24 with 1.43% strain

that the graphene sheets subjected to biaxial stress retain the strain along the zigzag C– C bonds. One can expect the surface adsorption of foreign atoms and molecules on the zigzag sites or at the top of the carbon atoms present at the junction of two zigzag and one armchair C–C sections. A gap of 0.214 eV is opened [see Fig. 1c] in this case in which the graphene is strained biaxially. As result , the semimetallic nature of graphene is changed resulting in a narrow gap semiconductor.

The calculations are repeated for 5%, 8.5% and 10% strains. The bandstructures corresponding to 5% uniaxial(along x and y directions) and biaxial strains are given in Figs. 2a,b & c, respectively. The direct band gap values are 0.41,0.58 &0.7 eV.

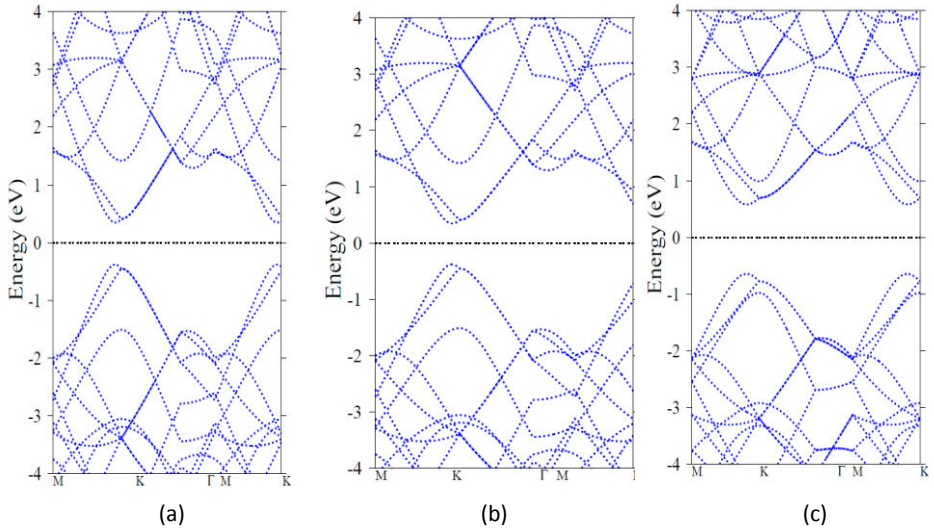

Fig. 2 Bandstructure of G24 with 5% strain

Similarly when the graphene sheet is subjected to a strain of 8% along the x- direction, the HOMO and LUMO separate at the "K" point leading to a gap (Figs. 3a) The bandstructure corresponding to 8% strain along the x- direction is depicted in Fig.3a. In this case the direct band gap is 0.8 eV.

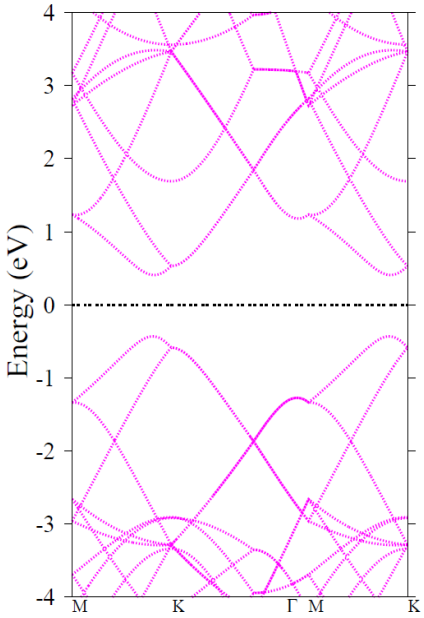

Fig. 3 Bandstructure of G24 under 8.5% strain

For 10% strain along the x- direction, *y*-direction and along *x*-*y* directions, the band structures are given in Figs. 4a,b & c. The corresponding band gaps are 1.1, 1.2 & 1.5 eV.
The first two are direct band gaps and the third one is a indirect band gap.

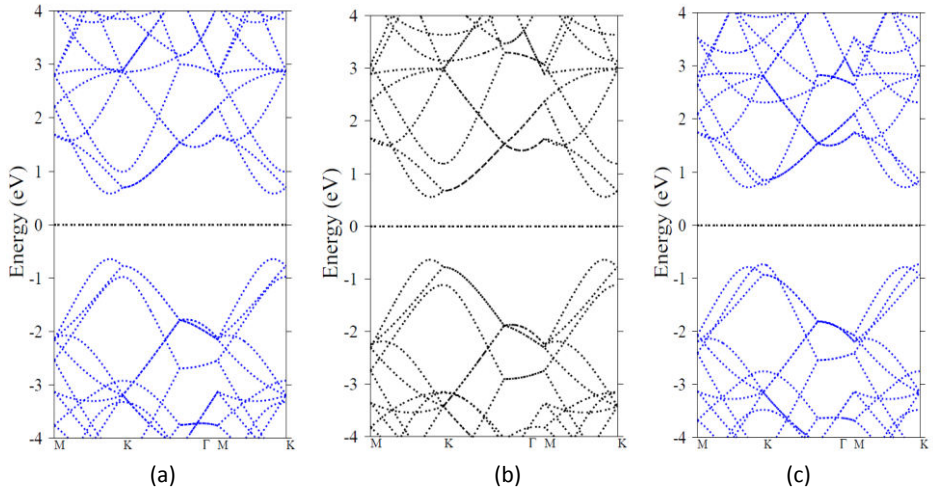

Fig.4 Bandstructure of G24 with 10% strain

The bandstructures for all the investigated graphene under stress are summarised in figs.5 and 6.

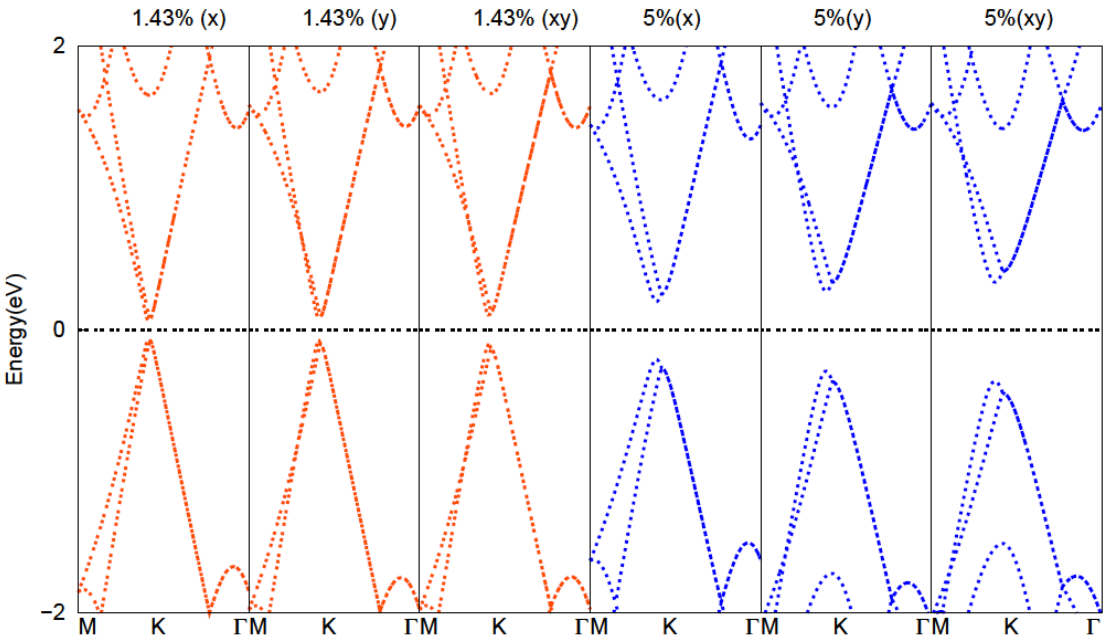

Fig. 5 Bandstructures G24 under strains 1.43% and 5%

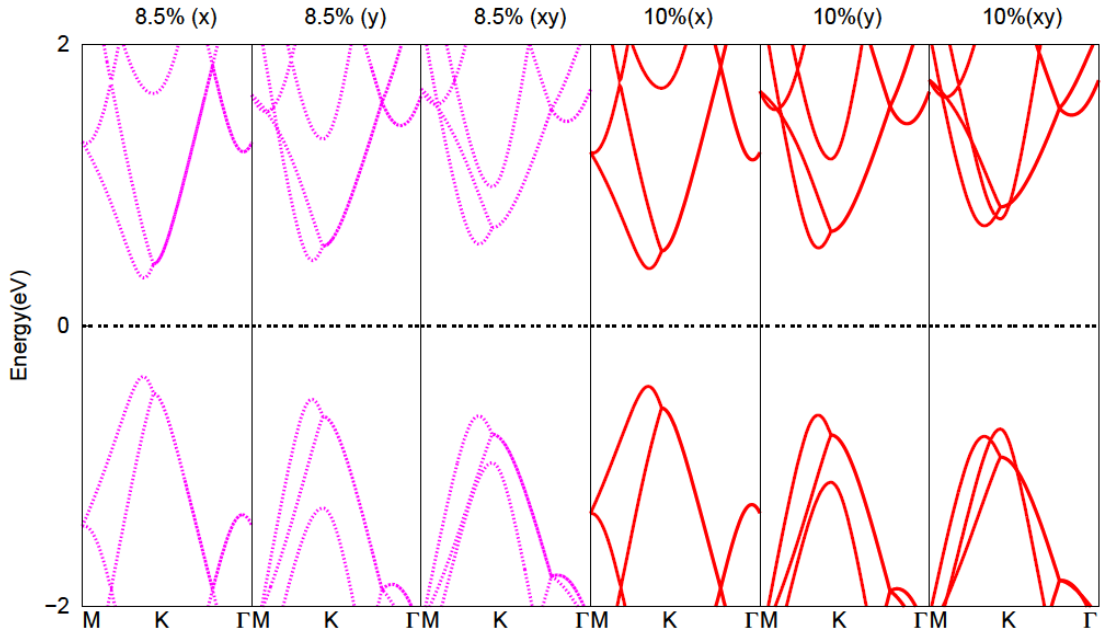

Fig. 6 Bandstuctures of G24 under strains 8.5% and 10%

For a biaxial strain (15%) a large direct band gap opens up at the K point (Fig. 7)

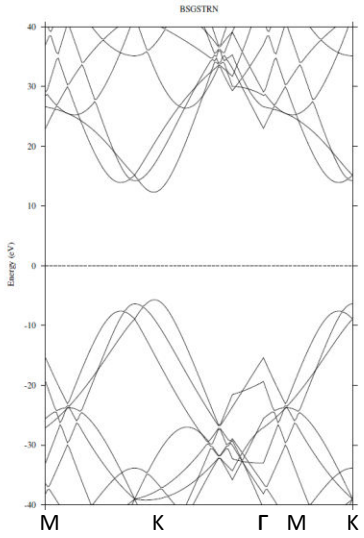

Fig. 7 Bandstucture of G24 under 15% strain

Possible mechanism for band gap opening under stain

Through strong σ bonds and delocalized π electrons the graphene layer is formed. The overlap of The vertically aligned p_z orbitals of carbon atoms in the hexagonal lattice overlap andresults in the formation of π orbitals. The π and π^* bands cross the Fermi level at a single point (K). Under strain the graphene the C–C bonds are elongated. The elongation in the C–C bonds due to the strain induces the localization [34] of π electron clouds (p_z orbitals) on the respective carbon atoms, reducing the overlap with the neighbours. Because of this the motion of carriers will be curtailed, thereby opening a band gap at the "K" point. One can also observe the reduction in the linear dispersion and rounded off (Dirac cones) energy bands near the K point [see Fig. 1c]. As a result, the velocity of massless Dirac fermions may drop down proportionatly not fully.. Under strained environment, Graphene, which is a semimetal, becomes a direct band gap semiconductor,of under the application of uniaxial or biaxial strain.

Summary and Goals achieved

In the past to open a gap in the bandstructure of graphene various techniques were tried and in some cases the gap opened up, but when the gap opens up the Dirac cones disappeared. Without Dirac cones graphene losses all its novelty. So opening a gap in graphene retaining Dirac cones has become a challenging task. We, through first principles study using Density Functional theory have done band gap tuning investigations by vacancy creation, substitutional doping, functionalization (surface doping) and strain engineering. We have succeeded in opening the band gap, retaining the Dirac cones in graphene through vacancy, adding impurity atom in the vacancy , substitutional co-doping, surface doping and strain engineering .

The outcome of the investigation are:

i) **In the case of graphene with single vacancy a direct band gap of ~ 1 eV is obtained. This is a spin polarized state.**

ii) **The graphene system with two monovacancie gives rise to an effective in direct band gap (pseudo gap) of ~ 1eV.**

iii) **The graphene substitutionally doped with B and N is co-doped (tri-doped) with S. This tri-doped (B,N,S) graphene has turned into a semiconductor (band gap ~1eV), with massless Dirac fermions and electrons contributing to its carrier mobility.**

iv) **Surface doping of various elements are tried and finally surface doping of sulpher is found to induce band gap opening in graphene. It moderately distorts the surface atoms and the interaction is limited such that a band gap opens without much distorting the Dirac cones. With single S a band gap of 1.4eV opens up.**

v) **Also when S is co-doped along with CO_2 or with NN similar band gap opening occurs.The calculation of surface doping of graphene with S is repeated with 96 atom simulation cell. The band gap value is 0.7 eV. The value of band gap can be tuned to the required value by varying the distance of S atom from the surface of graphene, which can be achieved by proper ion implementation technique.**

vi) **Finally bandgap opening in graphene is achieved through strain engineering. Our study suggests that this mechanism alter both structural and electronic properties of graphene. The combined action of structural modifications that involves stretching and compression of C–C bonds in the hexagonal network and charge localization mechanism are responsible for the gap opening in electronic spectrum of graphene. Even though is a nondestructive technique, the distortion to the Dirac cones are more compared to the other methods mentioned above.**

vii) **In all the above process the Dirac cones are retained to various extend ranging from 50% to 95% and the graphene is now a semiconductor with fast moving massless Dirac Fermions. These graphene semiconductors are better than the ordinary semiconductor because of the presence of Dirac cones with minimum distorsion and massless Dirac Fermions. This will have lot of application in device industry compared to a pristine graphene because of the presence of a gap and massless Dirac fermions contributing to its carrier mobility.**

viii) **As proposed in the project, We have computationally designed better performing, more sustainable and cost effective functionalized graphene material.**

Acknowledgements

The Principal investigator, Dr. K. Iyakutti is thankful to AOARD for the financial support through a project (**Grant FA2386-14-1-4007**). He also gratefully acknowledges SR16000 supercomputing resources from the Center for Computational Materials Science of the Institute for Materials Research, Tohoku University. The PI is thankful to the authorities of SRM University for providing necessary facilities to carry out the Project.

References

[1] A. K. Geim and K. S. Novoselov, *Nat. Mater.,* vol. 6, pp. 183–191, 2007.
[2] Wencai Ren & Hui-Ming Cheng, *Nature Nanotechnology* 9,726–730 (2014)
[3] Andrea C. Ferrari et al Nanoscale (2014) DOI: 10.1039/c4nr01600a
[4] Kostas Kostarelos & Kostya S. Novoselov, *Nature Nanotechnology* 9,744–745(2014)
[5] Emilie J. Siochi, "Graphene in the sky and beyond", *Nature Nanotechnology*9,745–747(2014)
[6] A memory for images, Elisa De Ranieri *Nano Lett.* 15, 259–265 (2015)
[7] "Ten years in two dimensions", *Nature Nanotech. 9,725(2014), Nature Nanotechnology* 9,737(2014)
[8] Withers F, Dubois M, Savchenko AK, *Phys Rev B* 2010, 82:073403-073407.
[9] Marc Dvorak et al, Scientific Reports,3:228 (2013) ,DOI:10.1038/srep02289
[10] Arramel, Andres Castellanos-Gomez and Bart Jan van Wees Graphene,2, 102-108,2013.
[11] S.M. Kozlov, F. Vines and A.Gorling, Adv. Mater.2011,23,2638-2643.
[12] M.F. Craciun, S. Russo, M. Yamamoto and S. Tarucha, Nano Today (2011) 6,42-60.
[13] Bi-Ru Wu and Chih-Kai Yang, AIP Advances 2, 012173 (2012).
[14] Ricardo Faccio et al, *J. Phys. Chem. C*, 2010, *114* (44), pp 18961–18971
[15] Castro Neto AH et al, The electronic properties of graphene. *Rev Mod Phys* 2009, 81:109-162.

[16] Boukhvalov DW, Katsnelson MI, *J Phys Condens Matter* 2009, 21:344205-344217
[17] R.M.Guzmán-Arellano et al, Appl. Phys. Lett. 105, 121606 (2014)
[18] Yanan Tang et al, J. Chem. Phys. 135, 224704 (2011); http://dx.doi.org/10.1063/1.36 66849
[19] Z. Xu and K. Xue, *Nanotechnology*, 21, 045704-1-7,2010.
[20] O.N.Ventura, Á.W. Mombrú, arXiv:1006.0589v1 [cond-mat.mtrl-sci cond-mat.mes-hall]June 4 2010.
[21] Ricardo Faccio, Alvaro W. Mombrú, arXiv:1312.5015v1[cond-mat.mtrl-sci] Dec 19 ,2013
[22] A. V. Krasheninnikov and R. M. Nieminen, *Theor.Chern. Ace.,* vol. 129, pp. 625–630,2011.
[23] H. Amara et al, *Phys. Rev. B,* vol. 76, pp. 115423-1–115423-10, 2007.
[24] F. Banhart, J. Kotakoski, and A. V. Krasheninnikov, *ACS Nano.,* vol. 5, pp. 26--41 , 2011.
[25] Beidou Guo et al Nano Ltt 10, 4975-4980 (2010)
[26] Yen-Chia Chen et al, *Nature Nanotechnology*(2015) doi:10.1038/nnano.2014.307
[27] Bernard R. Matis et al , *ACS Nano*, 2012, *6* (1), pp 17–22
[28] V. J. Surya, K. Iyakutti, H. Mizuseki, and Y. Kawazoe,IEEE- Trans. on Nanotechnology 11 (2012) 534-541
[29] K. Iyakutti, V. J. Surya, and Y. Kawazoe, AIP Conf. Proc. 1447, 293-294 (2012).
[30] V. J. Surya, K. Iyakutti, V. Prasanna Venkatesh, H. Mizuseki and Y. Kawazoe, Physica E 43 (2011) 1528-1534
[31] G. Kresse and J.Hafner, *Phys. Rev. B,* vol. 47, pp. 558–561, 1993.
[32] G. Kresse and J. Furthmuller, *Phys. Rev. B* . 54, pp. 11169– 11186, 1996.
[33] Peng Zhou et al, *Scientific Reports* 4, 6448, doi:10.1038/srep06448
[34] V.M.Pereira et al, Phys. Rev. Lett. 96, 036801-1-4,2006.